ULTRASONIC TEMPORARY SOFTENING AND RESIDUAL HARDENING

Ali H. Alhilfi[1] **– Andrew Rusinko**[2*]

[1] Misan University, Iraq
[2] Donát Bánki Faculty of Mechanical and Safety Engineering, Obuda University, Nepszinhaz St. 8, Budapest, Hungary, H-1081

ARTICLE INFO

***Article history*:**
Received: 30.08.2021.
Received in revised form: 31.03.2022.
Accepted: 31.03.2022.

Keywords:
Ultrasound
Plastic deformation
Residual hardening

DOI: https://doi.org/10.30765/er.1869

Abstract:

The present paper aims to model ultrasonic effects such as temporary softening and residual hardening. While temporary softening is observed during simultaneous action of mechanical forces and ultrasound, residual hardening manifests itself after switching off the ultrasound. The analytical description of these phenomena is conducted in terms of the synthetic theory of irrecoverable deformation. The model results show good agreement with experimental data obtained for the ultrasound-assisted compression of pure aluminum.

1 Introduction

Nowadays, ultrasonic technology is a convenient and accessible tool to assist many metalworking processes, such as forming, welding, and microelectronic wire bonding. Ultrasound has various advantageous characteristics: high reliability and current carrying capacity, "cold process", short process time, comparatively low energy consumption, etc. For this reason, acoustoplasticity has gained much interest in science and industry.

There are three central phenomena associated with acoustic energy and its effect on the deformation properties of metals [1]-[9]:

(i) Stress-drop recorded at the moment as ultrasound is On.
(ii) Ultrasonic temporary softening caused by ultrasound when unidirectional and oscillatory loading are applied simultaneously (acoustoplasticity) - the material flows at lower stress than when mechanical loading alone is applied.
(iii) Ultrasonic residual hardening or softening detected after ultrasound is turned off - the development of plastic deformation of the material deformed after sonication requires greater (hardening) or lesser (softening) stress than normal plastic deformation.

For decades, numerous studies have been conducted to improve the understanding of the factors that determine the above phenomena. Nevertheless, the problem is far from being solved. Nevertheless, it is possible to use dislocation theory to design a deformation mechanism that explains the elongation of metals in the presence of ultrasound.

With *temporary ultrasonic softening*, there are the following suggestions about the effects of acoustic energy.

1. Malygin [1] proposed a stress superimposition mechanism, implying that ultrasonic waves activate blocked dislocations hardened under ordinary deformation and decrease stresses for further plastic deformation. The microstructure includes an increase in dislocation density and the formation of blocked loops of vacancies (it is worth noting that the separation of the ultrasonic defects from those of unidirectional loading can be complicated [2]. However, Daud et al. [3] found that the simple addition of unidirectional and oscillatory stresses leads to incorrect results, i.e., a more nuanced approach is needed.

* Corresponding author
E-mail address: ruszinko.endre@uni-obuda.hu

2. Localized heating produced by acoustic energy may also be sufficient to produce some annealing of the microstructure. Deshpande et al. [4] draw an analogy between the effects of hot deformation and ultrasound action and indicate that similar microstructure evolution results can be observed when thermal energy is replaced with ultrasonic energy. As a result, numerous investigators (e.g. [2], [5]-[7]) suggest that ultrasonic vibration induces sufficient heat input to the sample to initiate dynamic annealing, which leads to the reduction of dislocation density.

The mechanism of dynamic annealing mainly depends on the stacking fault energy (SFE) of sonicated material. According to Deshpande et al [4], [8], although aluminum and copper have the same FCC crystal structure, they recover through different annealing mechanisms (polygonization and recrystallization, respectively), resulting in a significantly different microstructure after deformation in the presence of ultrasonic energy. Metals with low SFE (e.g., copper, titanium, gold) soften mainly by recrystallization, in which the rapid migration of grain boundaries intensively "cleans" the deformed matrix. For high SFE materials such as aluminum, the main microstructural evolution during dynamic recovery is the extinction of dislocations of opposite sign and the rearrangement of free dislocations into subgrains surrounded by grain boundaries of low angle, i.e., aluminum is softened by polygonization.

Kulemin [9] summarizes the stated above: when external loading is applied along with ultrasonic irradiation, both hardening and softening occur, but the former is more intensive than the latter, and as a result, we observe the phenomenon of temporary softening. This expression is correct, but there is a lack of consideration of the influence of the defect structure formed during the acoustic plasticity on the plastic properties of the material after the US is switched off.

Residual ultrasonic effects. The material's deformation properties that have undergone acoustoplasticity depend entirely on the microstructure developed during plastic deforming in the acoustic field. According to Lum [2], the residual acoustic effect is attributed to the net balance between dynamic annealing and the multiplication of dislocations. It is suggested that the appearance of acoustic residual softening or hardening is determined by the net result of ultrasonic effects on the internal structure of the materials, especially dislocation density. On this basis, we attribute the residual softening to the dominating role of recrystallization during acoustoplasticity, whose "cleaned" structure exerts fewer restrictions against the development of plastic deformation after the US is off. On the other hand, if the dynamic annealing mechanism manifests itself via polygonization, the dislocation net hardens the material. Therefore, at least for pure metals, we propose to relate the appearance of residual softening or hardening to the value of SFE, which governs the recovery mechanisms and, in this end, determines the potential opposing effect on activating and multiplying dislocations.

This paper aims to give an analytical description of the following ultrasonic effects: a) ultrasound-induced stress drop, b) ultrasonic temporary softening, and c) ultrasonic residual hardening. For the mathematical apparatus, the synthetic theory of irrecoverable deformation is utilized. The present research extends the previously obtained results [10] that deal with ultrasonic softening alone.

2 Synthetic theory

In terms of this theory [12], the plastic deformation at a point of the body (plastic strain vector, $\boldsymbol{e}$, in three-dimensional stress deviator stress S^3) is calculated as a sum of plastic shifts in active slips systems, i.e., where the resolved shear stress exceeds the material yield strength (the Schmidt law):

$$\boldsymbol{e} = \iiint_V \varphi_N \boldsymbol{N} dV, \tag{1}$$

where φ_N – plastic strain intensity – is an average measure of plastic deformation within one slip system; unit vector $\boldsymbol{N}$ gives an orientation of slip systems; dV is an elementary set of the slip systems involved in plastic deformation.

A vital feature of the synthetic theory is the formulation of yield criterion and strain hardening rule. Namely, we work not with a yield surface itself but with its tangent planes, i.e., the yield surface is treated as an inner envelope of the tangent planes. The physical sense of the tangent planes is that every tangent plane corresponds to a slip system at the point of the body. The positions of planes are defined via their distances

(H_N) and unit normal vectors ($\boldsymbol{N}$). Therefore, the Von-Mises yield criterion adopted in the synthetic theory is treated as a set of equidistant planes for all directions, $H_N = S_S$ (Figure 1a). A stress vector presents loading ($\boldsymbol{S}$). In the course of loading, the stress vector moves (shifts) at its endpoint (load point) a set of planes from their initial position.

The movements of the planes located on the endpoint of the vector $\boldsymbol{S}$ are translational, i.e., the plane orientations remain unchangeable. The planes that are not on the endpoint of the vector $\boldsymbol{S}$ remain unmovable. The displacement of a plane on the endpoint of the stress vector symbolizes a plastic flow within the corresponding slip system (φ_N). Figure 1b shows the loading surface for the case of uniaxial tension.

It consists of two parts: a) sphere constructed as the envelope of motionless planes, and b) a cone whose generators are formed by the boundary planes shifted by the vector $\boldsymbol{S}$. The planes shifted by the vector $\boldsymbol{S}$ during loading are located on the top of this cone.

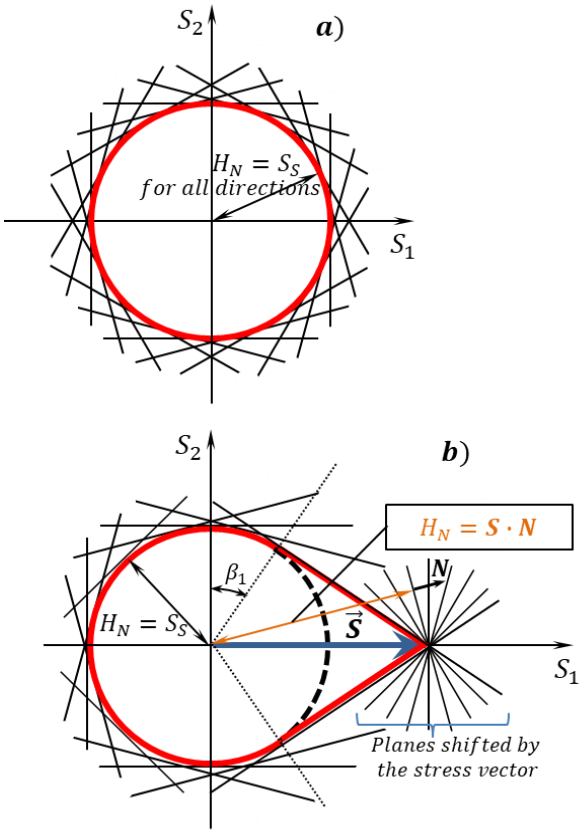

Figure 1. Yield (a) and loading surface (b) for uniaxial tension in terms of the synthetic theory in the S_1-S_2 coordinate plane (angle β_1 gives the orientation of the boundary planes shifted by the stress vector).

Now, we can define the plastic strain intensity – and indeed the plastic flow rule on the microlevel of material – as [12]

$$r\varphi_N = H_N^2 - S_S^2 = \begin{cases} (\boldsymbol{S}\cdot\boldsymbol{N})^2 - S_S^2 & \text{for planes reached by } \boldsymbol{S}:\ H_N = \boldsymbol{S}\cdot\boldsymbol{N} \\ 0 & \text{for planes not reached by } \boldsymbol{S}:\ H_N > \boldsymbol{S}\cdot\boldsymbol{N} \end{cases}. \tag{2}$$

The scalar product $\boldsymbol{S}\cdot\boldsymbol{N}$ defines the resolved shear stress acting in one slip system. The plane distance H_N reflects the material's hardening because the greater the distance, the greater stress is needed to reach the plane. In Eq. (2), $S_S=\sqrt{2/3}\sigma_S$, where σ_S is the yield strength of the material; r is the model constant determining the slope of stress~strain curves; $[r]=\mathrm{MPa}^2$.

Consider the case of compression. Since, in terms of the synthetic theory, isotropy postulate holds, the results obtained for uniaxial tension [10], [12] can also be utilized for compression. So, the loading is represented by $\boldsymbol{S}\left(\sqrt{2/3}\sigma,0,0\right)$ stress vector that elongates along the S_1 axis. Eqs. (1) and (2) take the following form [12]

$$\varphi_N=\frac{1}{r}\left(S_1N_1-S_S\right)^2=\frac{2}{3r}\left[\left(\sigma\sin\beta\cos\lambda\right)^2-\sigma_S^2\right], \tag{3}$$

where angles β and λ give the orientation of vector $\boldsymbol{N}$ in S^3 [12].

Now the plastic deformation vector component (e) is calculated via (1) as

$$e=\frac{4\pi}{3r}\int_{\beta_1}^{\pi/2}\int_{0}^{\lambda_1}\left[\left(\sigma\sin\beta\cos\lambda\right)^2-\sigma_S^2\right]\sin\beta\cos\lambda\cos\beta\,d\lambda\,d\beta=a_0\Phi\left(b\right), \tag{4}$$

Where

$$a_0=\frac{\pi\sigma_S^2}{9r},\quad \Phi\left(b\right)=\frac{1}{b^2}\left[2\sqrt{1-b^2}-5b^2\sqrt{1-b^2}+3b^4\ln\frac{1+\sqrt{1-b^2}}{b}\right],\quad b=\frac{\sigma_S}{\sigma}. \tag{5}$$

The integration boundaries in (4) are obtained from (3) by letting $\varphi_N=0$ and $\lambda=0$:

$$\sin\beta_1=\frac{\sigma_S}{\sigma},\quad \cos\lambda_1=\frac{\sigma_S}{\sigma\sin\beta}. \tag{6}$$

If to add σ/E to e from (4), we obtain the total deformation at the stress σ (E is the Young modulus of material).

3 Extension of the Synthetic Theory to the case of plastic straining in the presence of ultrasound

In order to model the effects of ultrasound on the plastic straining of metals, we extend Eq. (2) for the plastic strain intensity in the ultrasonic field (φ_{NU}) by two terms, U_t and U_r, which reflect the ultrasonic temporary softening and residual hardening, respectively:

$$r\varphi_{NU}=H_N^2+U_t^2-h\left(\varepsilon-U\right)U_r^2-S_S^2, \tag{7}$$

where h is the Heaviside step function and U is ultrasonic energy density $\mathrm{J/m^3}$. The ultrasonic energy is readily expressed via vibration- or stress-amplitude (ξ and σ_m respectively: $U=\left(1/2\right)\rho\xi^2\omega^2$ and $\sigma_m=E\xi\omega/c$ [16], where ρ is the density of a material, ω is the angular frequency of vibration).

As for ε, it has the same unit as U and we define it as $\varepsilon>0$ and $\varepsilon\to 0$. As will be seen below, the only role of $h\left(\varepsilon-U\right)$ function is to separate the effect from U_t and U_r.

3.1 Temporary softening

It is easy to see that we have $\varepsilon - U < 0$ and $h(\varepsilon - U) = 0$ during plastic deforming coupled with ultrasound. Consequently, Eq. (7) yields the following form

$$r\varphi_{NU} = H_N^2 + U_t^2 - S_S^2 \qquad \text{during acoustoplasticity } (U > 0). \tag{8}$$

The term U_t reflects the ultrasonic temporary softening because its appearance with a positive sign in Eq. (8) makes it possible to maintain a given value of the strain intensity at less value of the unidirectional stress involved into $H_N = \boldsymbol{S} \cdot \boldsymbol{N}$. In other words, the plastic deformation in the ultrasonic field develops at lower stress due to the compensation from acoustic energy.
We define U_t as

$$U_t = A_1 U^{A_2} \left(2 - e^{-pt}\right)(\boldsymbol{u} \cdot \boldsymbol{N}), \quad t \in [0, \tau], \tag{9}$$

where τ is the sonication duration and $\boldsymbol{u}$ is a unit vector indicating the vibration mode (longitudinal, torsional, etc.). For longitudinal sonication, the $\boldsymbol{u}$ vector has $(1,0,0)$ coordinates in S^3. If to denote through $\boldsymbol{U}$ the vector $A_1 U^{A_2}\left(2 - e^{-pt}\right)\boldsymbol{u}$, Eq. (9) becomes $U_t = \boldsymbol{U} \cdot \boldsymbol{N}$, i.e., the action of ultrasound is presented by a vector whose component depends on acoustic energy/vibration amplitude and time.

Eq. (9) correctly reflects numerous studies' results carried out on many metals (zinc, cadmium, aluminum, copper, and steel [5], [2], [11], [13]-[15]. They report that the magnitude of ultrasonic temporary softening depends on the vibration/stress amplitude. We relate the temporary softening effect to the ultrasonic energy (stress amplitude) via power function $A_1 U^{A_2}$. Further, the product $A_1 U^{A_2} e^{-pt}$ reflects the temporary multiplication of ultrasound-induced defects (ψ_{NU}), proposed in Rusinko's early work (2011). The e^{-pt} function reflects the well-known fact that the number of ultrasound defects first increases with time and then reaches a plateau [9], [10], [17]. Therefore, Eq. (9) is dual. On the one hand, the ultrasound defects harden the material, but, on the other hand, they become centers of softening processes. As evident from (9), since the term $\left(2 - e^{-pt}\right)$ is always positive, the net effect is the prevalence of softening mechanisms during unidirectional and oscillating load simultaneous action.

Formulae (8), (9), and (1) describe the plastic deformation superimposed by ultrasound, portions $C_1 - C_2 - C_3$, or $B_1 - B_2 - B_3$ in Fig. 2. $C_1 - C_2$ and $B_1 - B_2$ are the stress drops at the instant as ultrasound On. $C_2 - C_3$ and $B_2 - B_3$ are the diagram portions in the acoustic field. It must be noted that, according to Yao et al. [11], the magnitude of the stress drop depends on the value of the stress when the US is On – $\Delta\sigma_{B_1B_2} > \Delta\sigma_{C_1C_2}$ (approximately 52.46 MPa vs. 44.45 MPa [11]) – at the same intensity of ultrasound applied. Therefore, the greater stress is acting, the more significant effect from the sonication can be expected. In other words, the greater deformation energy accepts the additional ultrasonic one, the more remarkable softening occurs.

The A_2A_3 and B_2B_3 portions show identical tendencies – the simultaneous action of unidirectional and vibrating stresses results in smaller stress values needed to continue the plastic deforming.

The consideration of Eqs. (8)-(9) and Figure 2 makes it possible to analyze the quantities (model constants) A_1, A_2, and p from (9). The function $A_1 U^{A_2} e^{-pt}$ governs the stress drop caused by the ultrasound ($t = 0$) and the kinetics of the $\sigma \sim \varepsilon$ diagram in the acoustic field $t \in (0, \tau]$. To catch the fact that this drop depends on the value of unidirectional stress when the US is On, we define A_1 as an increasing function of static stress:

$$A_1 = A_1'\left(1 + a_1 f(\sigma)\right) \tag{10}$$

where $f(\sigma)$ is a linear function of the static stress, its concrete form is presented in the paper's final section. So, to plot the ultrasound-assisted stress-strain diagram, we need to choose the following four model constants: A_1', a_1, A_2, and p. The constants A_1', a_1, and A_2 govern the magnitude of the stress drop as a function of ultrasound intensity and the point where the ultrasound is On. The model constant p is responsible for the slope of the stress-strain diagram in the acoustic field. We choose these constants so to fit in the best way experimental data.

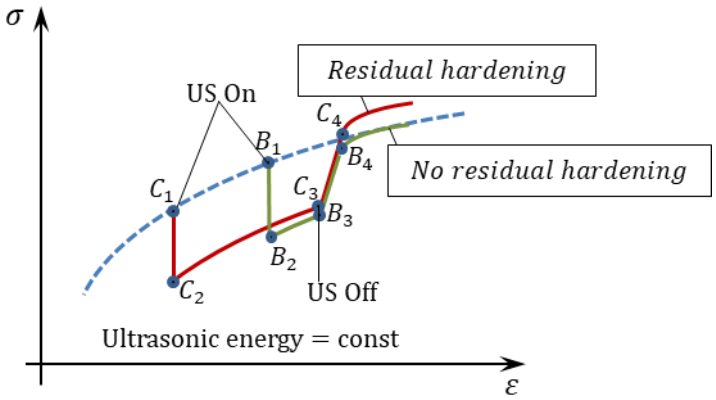

Figure 2. Schematic stress~strain diagrams with the sonications of different duration (according to [11]).

3.2 Residual hardening

Consider the plastic strain intensity after the ultrasound is Off. Since at $U=0$ we have $U_t=0$ and $h(\varepsilon)=1$, Eq. (7) takes the following form

$$r\varphi_{NU}=H_N^2-U_r^2-S_S^2 \qquad \text{after the ultrasound is Off } (t>\tau,\ U=0) \tag{11}$$

The term U_r, which stands with a negative sign in Eq. (11), suppresses the development of plastic slips φ_{NU}, i.e., it is responsible for ultrasonic hardening. We define U_r as

$$U_r=A_3\int_0^{\tau}U^{A_4}dt, \tag{12}$$

Again, we propose a power function to express the dependence of ultrasonic residual hardening upon the ultrasound intensity with model constants A_3 and A_4. At the same time, the intensity of sonication is not the only parameter governing the magnitude of the hardening effect. Namely, the sonication duration also plays an important role; in other words, the time-integral in (12) reflects the time-dependent magnitude of ultrasonic energy injected into the material. Therefore, the term U_r reflects a post-sonicated-defect pattern leading to material characteristics/response changes after the acoustoplasticity. Figure 3 demonstrates the temporary behavior of functions U_t and U_r from Eqs. 7, (9), and (12), respectively.

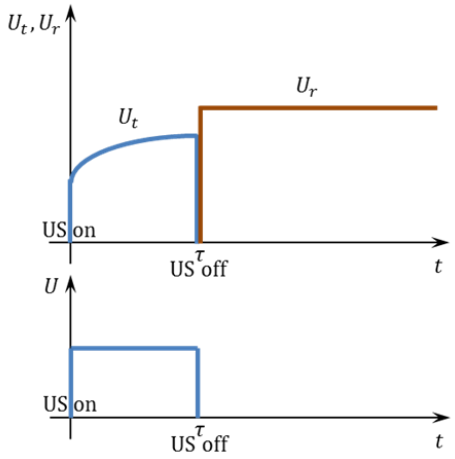

Figure 3. Temporary and residual terms in Eq. (7) as a function of ultrasonic action.

Eqs. (9), (10), and (1) model the development of deformation from points C_3 and B_3 in Figure 2. To apply these equations, one must choose the model constants A_3 and A_4 to ensure the best agreement between the model and experimental results.

As the ultrasound is off (points C_3 and B_3), the plastic deformation starts after elastic portions C_3C_4 and B_3B_4. The elastic deforming continues until the value of φ_N remains negative in (11) due to the presence of U_r. The resumption of plastic deformation starts as φ_N becomes positive, but even in this case, greater stress value is needed to develop the plastic deformation. This conclusion follows from the comparison of Eqs. (11) and (2) – $\varphi_{NU} < \varphi_N$ as the ultrasound is Off.

That is the essence of ultrasonic residual hardening. Another interesting fact is that this phenomenon strongly depends, among other things, upon the sonication duration (8 sec for C_2C_3 and 2 sec for B_2B_3). If the ultrasound is off at points C_3, i.e., after eight seconds of sonication, the plastic straining develops at a higher stress level than at ordinary loading. At the same time, the plastic straining, which follows two-second sonication, returns on $\sigma \sim \varepsilon$ curve corresponding to the ordinary loading. Therefore, not only the US intensity but also its duration influences the post-sonicated material behavior. To put this another way, if the ultrasound energy, roughly speaking the product of US intensity and sonication time, does not provide substantial changes in the defect structure of the material, the residual effects are not observed.

4 Uniaxial compression

This section shows how the relationships presented in the previous section, formulae of Synthetic theory extended to the case of the ultrasound-assisted plastic deformation, work for the case of uniaxial compression.

4.1 As vibration starts, formulae (8) and (9) at $t = 0$ give

$$r\varphi_{NU} = \left(\boldsymbol{S}\cdot\boldsymbol{N}\right)^2 + \left[A_1U^{A_2}\left(\boldsymbol{u}\cdot\boldsymbol{N}\right)\right]^2 - S_S^2 = \frac{2}{3}\left[\left(\sigma_U\sin\beta\cos\lambda\right)^2 + \frac{3}{2}\left[A_1U^{A_2}\sin\beta\cos\lambda\right]^2 - \sigma_S^2\right] \qquad (13)$$

The boundary angles β and λ where $\varphi_{NU} = 0$ are

$$\sin\beta_{1U} = \frac{\sigma_S}{\sqrt{\sigma_U^2 + \frac{3}{2}\left(A_1U^{A_2}\right)^2}} \equiv b_U, \quad \cos\lambda_{1U} = \frac{\sigma_S}{\sqrt{\sigma_U^2 + \frac{3}{2}\left(A_1U^{A_2}\right)^2}\sin\beta}. \qquad (14)$$

To ensure the stress drop at the constant deformation value (portions C_1C_2 or B_1B_2 in Figure 2), we demand that $\varphi_{NU} = \varphi_N$ at the same set of planes where the strain intensity is positive ($\beta_{1U} = \beta_1$, compare Figsure 4a and 4b). Equating b_U to b from (14) and (6) yields the value of stress (σ_U) maintaining the same deformation as before the US was On:

$$\sigma_U = \sqrt{\sigma^2 - \frac{3}{2}\left(A_1 U^{A_2}\right)^2}. \tag{15}$$

The formula above enables us to calculate the ultrasound-induced stress drop.

As seen from Figure 4b, the loading surface preserves its shape due to the compensation element $\boldsymbol{U}$, i.e., less value of unidirectional stress is needed to keep the deformation at the instant as the ultrasonic vibration starts.

4.2 During the simultaneous action of unidirectional loading and ultrasound (portions C_2C_3 or B_2B_3 in Figure 2), Eq. (9) gets

$$r\varphi_{NU} = \frac{2}{3}\left[\left(\sigma_U \sin\beta\cos\lambda\right)^2 + \frac{3}{2}\left[A_1 U^{A_2}\left(2 - e^{-pt}\right)\sin\beta\cos\lambda\right]^2 - \sigma_S^2\right] \quad t \in [0, \tau]. \tag{16}$$

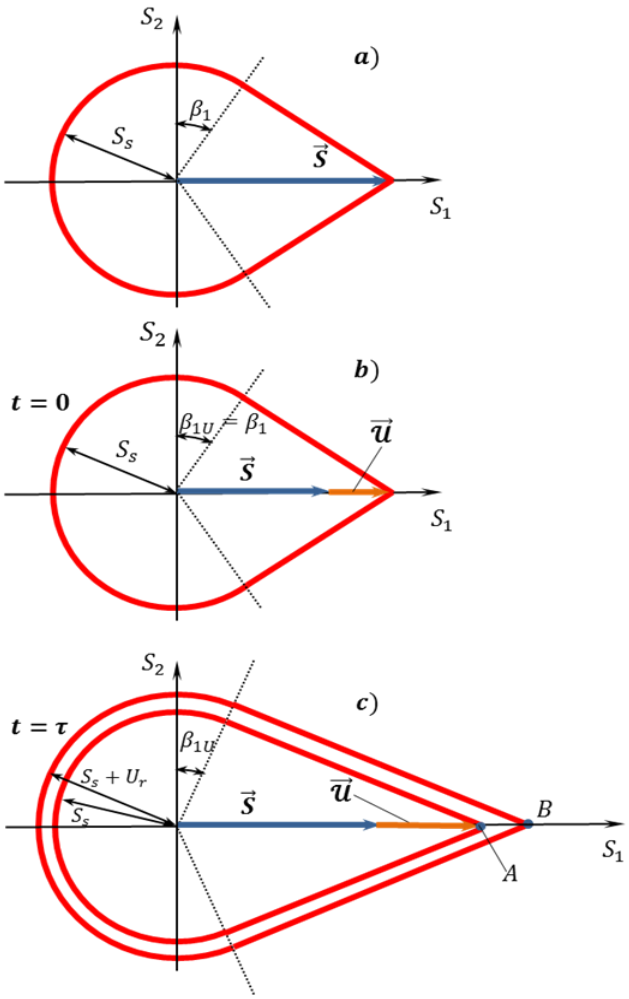

Figure 4. Evolution of loading surface during the sonication (tangent planes are not shown): a) before the sonication; b) the first moment as US is On; c) the end of sonication.

Plastic deformation in acoustoplasticity (e_U) is calculated by Eq. (1) with the integrand from (16). As a result,

$$e_U = a_0 \Phi\left(b_u\right), \quad b_U = \frac{\sigma_S}{\sqrt{\sigma_U^2 + \frac{3}{2}\left(A_1 U^{A_2}\left(2 - e^{-pt}\right)\right)^2}}. \tag{17}$$

Again, comparing Eq. (17) to (6), we can see that the presence of ultrasonic energy requires less stress to develop the plastic deformation of a specimen. The inner surface in Figure 4c, which corresponds to the end of sonication, clearly demonstrates that the common action of static ($\boldsymbol{S}$) and acoustic ($\boldsymbol{U}$) vector-portions reaches the loading point A.

Eqs. (13)-(15) describe the phenomenon of temporary ultrasonic softening analytically.

4.3 After US is off ($t > \tau$), $U_t = 0$ and $U_r > 0$ (Figure 3). Compared to (9), the plastic strain intensity (11) loses the term U_t, which facilitated the strain intensity, but includes U_r of negative sign. As a result, the plastic strain intensity becomes of negative sign, i.e., the development of plastic deformation ceases (portions C_3C_4 or B_3B_4 in Figure 2). Eqs. (11) and (12) give that

$$H_N^2 = r\varphi_{NU} + \left[A_3 U^{A_4}\tau\right]^2 + S_S^2, \tag{18}$$

where φ_{NU} is the plastic strain intensity accumulated during the acoustoplasticity. Eq. (18) says that when ultrasound is Off, the distances obtain jump-wise increments in all directions by the magnitude of U_r (Fig. 4c). Therefore, now, the endpoint of the stress vector is inside the loading surface, and plastic deformation will resume only when the stress vector reaches the first tangent plane, point B. In other words, till the plastic strain intensity from (11) and (12),

$$r\varphi_{NU} = \frac{2}{3}\left[\left(\sigma \sin\beta\cos\lambda\right)^2 - \frac{3}{2}\left(A_3 U^{A_4}\tau\right)^2 - \sigma_S^2\right] \quad \left(\sigma > \sigma_U\right), \tag{19}$$

remains negative, we have only an elastic deformation increment, corresponding to the linear portions C_3C_4 or B_3B_4 in Figure 2. If to compare (19) to (2), it is clear that material has been harder after the sonication, i.e., more significant stresses are needed to develop the same deformation as for the basic $\sigma \sim \varepsilon$ diagram. This fact reflects the phenomenon of ultrasonic residual hardening.

The increment in plastic strain intensity ($\Delta\varphi_{NU}$), after the elastic portion (stress-strain diagrams beyond points C_4 or B_4 in Figure 2), is calculated as the difference of strain intensities from Eqs. (19) and (16)

$$\Delta\varphi_{NU} = \frac{2}{3r}\left\{\left(\sigma \sin\beta\cos\lambda\right)^2 - \left[\left(\sigma_U \sin\beta\cos\lambda\right)^2 + \frac{3}{2}\left[A_1 U^{A_2}\left(2 - e^{-p\tau}\right)\sin\beta\cos\lambda\right]^2\right] - \frac{3}{2}\left(A_3 U^{A_4}\tau\right)^2\right\}, \tag{20}$$

where σ_U is the value of stress at $t = \tau$.

Plastic strain increment (Δe) after the elastic portion is calculated by Eq. (1) as

$$\Delta e = \frac{2\pi}{r}\int_{\beta_2}^{\pi/2}\int_{0}^{\lambda_2} \Delta\varphi_{NU} \sin\beta\cos\lambda\cos\beta\, d\lambda\, d\beta. \tag{21}$$

The integration boundaries in (21) are determined from Eq. (19) at $\varphi_N = 0$ and $\lambda = 0$. It is because the movements of planes on the endpoint of the stress vector for the range $\beta_2 \le \beta \le \beta_{1U}$ start from the sphere of radius $S_S + U_r$ (Figure 5).

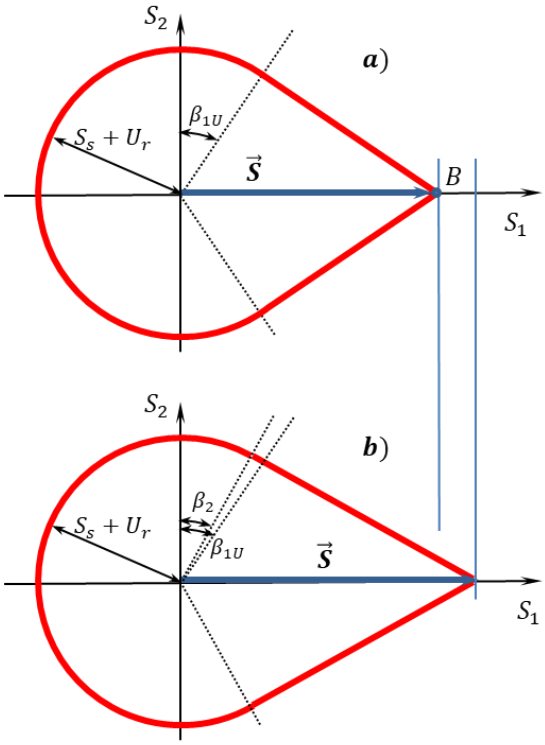

Figure 5. Evolution of loading surface after the sonication (point B is from Figure 4): a) the start of plastic deforming after the elastic portion; b) plastic deforming under the residual hardening.

So

$$\sin\beta_2 = \frac{\sqrt{\sigma_S^2 + \frac{3}{2}\left(A_3 U^{A_4}\tau\right)^2}}{\sigma}, \quad \cos\lambda_2 = \frac{\sqrt{\sigma_S^2 + \frac{3}{2}\left(A_3 U^{A_4}\tau\right)^2}}{\sigma\sin\beta}. \tag{22}$$

Therefore, starting from the instant as US is Off, the total deformation takes the following form

$$e = e_U + \Delta e + \frac{\sigma}{E}. \tag{23}$$

where e_U is calculated via (17) at the end of sonication ($t = \tau$).

In sum, the plastic deformation for the post-sonicated period is calculated via Eqs. (20)-(23), where constants A_3 and A_4 must be chosen to achieve the best fit between the experimental and model stress~strain curves. These constants regulate the increase in the stress needed to continue the plastic deforming after US is Off.

5 Results and discussion

Here, our goal is (**i**) to construct model stress~strain curves in the compression tests for pure aluminum according to the sonication regimes shown in Figure 2, (**ii**) to compare the analytic results with those obtained

experimentally by Yao et al. [11]. The Young modulus and yield strength of pure aluminum are taken as $E = 68$ GPa , and $\sigma_S = 45$ MPa , respectively. The value of the σ_S is read from the experimental curve in Figure 6.

A) First, we choose the constant model r to fit the ordinary (base) $\sigma \sim \varepsilon$ diagram to the experimental one as best as possible. The analytic $\sigma \sim \varepsilon$ curve from Figure 6, which is plotted via Eqs. (4)-(6) at $r = 1.3 \times 10^4$ MPa^2 shows good agreement with experimental data.

B) The next step is the instant when US is on. We utilize Eq. (15) to calculate the ultrasound-induced stress drop – the intensity of ultrasonic energy is $U = 126.6$ J/m^3 , the ultrasonic vibration starts at $\sigma_1 = 93.9$ MPa [11] (point **1** in Figure 6).

Let us define A_1 from (10) in a linear manner as

$$A_1(\sigma) = A_1' \left(1 + a_1 \frac{\sigma}{\sigma_1} \right). \tag{24}$$

We propose the following values of the model constants: $A_1' = 18.5$ m^3/J , $a_1 = 0.205$, and $A_2 = 0.25$. Formula (15) with these constants lead to the correct result (point **2** in Figure 6).

C) Further, Eq. (17) serves as an analytical tool to plot $\sigma \sim \varepsilon$ diagram under the action of ultrasound lasting $\tau = 8$ s (portion **2-3** in Figure 6). The utilization of this formula requires the four model constants, A_1' , a_1 , A_2 , and p . The values of the first three constants are the same as above and the constant p we propose as $p = 0.034$ s^{-1}. Again, it can be stated that agreement between the model and test results has been achieved.

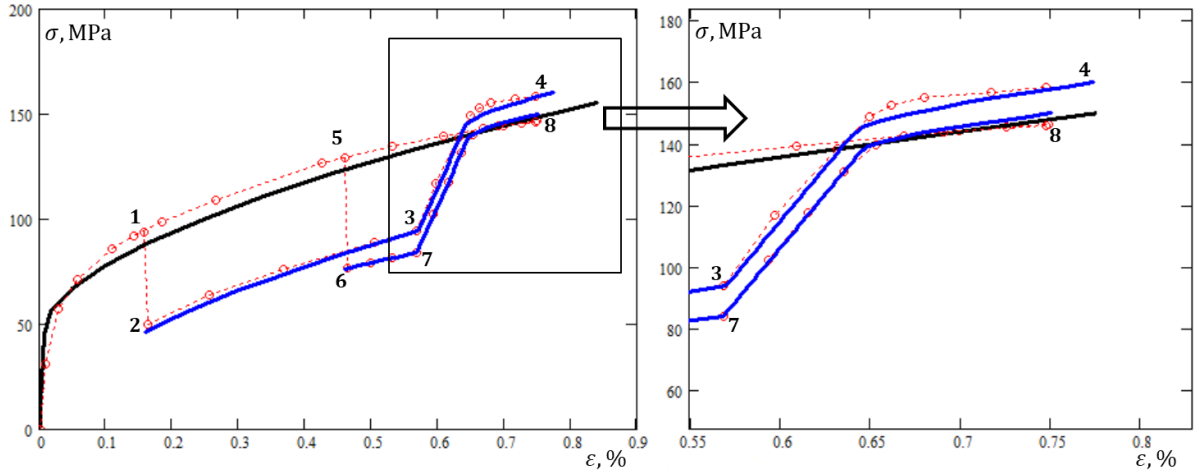

Figure 6. Vibration-assisted stress~strain diagrams of aluminum; lines – model, ○ – experiment [11].

D) Finally, the plastic deformation of post-sonicated material – portion **3-4** in Figure 6. This portion is plotted via Eqs. (20)-(23). Preserving the values of the model constant proposed in the last portions, one must choose the values for A_3 and A_4 . We choose $A_3 = 3.5 \times 10^{-7}$ m^3/J and $A_4 = 4$, which leads to a satisfactory result.

E) To test the model constants proposed above, we utilize Eq. (15) to calculate the ultrasound-induced stress drop for different values of ultrasonic energy: $U_k = 5.89,\ 22.0,\ 60.33,\ 126.6$ J/m^3 (US is on at $\sigma_1 = 93.9$ MPa). Figure 7, plotted via Eq. (15), demonstrates that the model constants chosen at point **B)** lead to the magnitudes of stress drops for different U_k correlating well with the experiment.

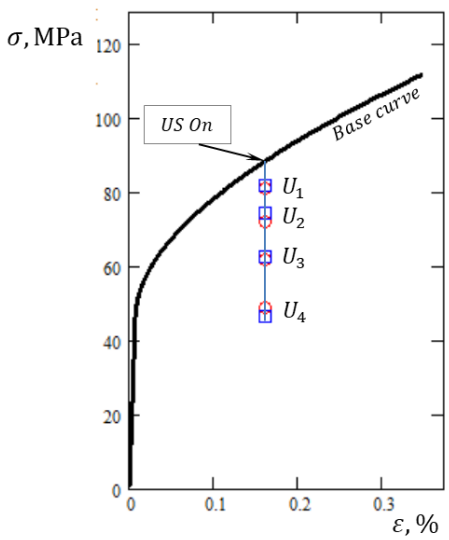

Figure 7. Stress-drop due to different values of ultrasound energy U_k (k=1,...,4). Material – aluminum; □ – model, ○ - experiment [11].

F) Let us inspect whether the constant models from points **A)-D)** give correct results for another sonication mode. Consider the case when ultrasound of the same intensity as in **A)-D)** ($U = 126.6\ \mathrm{J/m^3}$) starts when $\sigma_5 = 128.7$ MPa (point **5** in Figure 6) and acts only for 2 seconds ($\tau = 2$ s). As discussed in the Introduction, the amount of deformation impacts the magnitude of the stress drop caused by acoustic energy.
This phenomenon finds its place in Figure 6 via different stress-drop values: $\Delta\sigma_{5-6} > \Delta\sigma_{1-2}$. It is this fact that forced us to define A_1 as a function of acting stress, Eqs. (10) and (24). Since it is evident that $A_1(\sigma_5) > A_1(\sigma_1)$, Eq. (15) gives a greater stress-drop **5-6** in Figure 6 compared to **1-2** observed at σ_1. The deformation along **5-6-7-8** in Figure 6 is plotted through the same formulae and constants as in points **A)-D)**. As seen from Figure 6, the sonication of duration $\tau = 2$ s leads to a negligible deviation from the base $\sigma \sim \varepsilon$ diagram after the ultrasound is Off. This is because the term $A_3 U^{A_4} \tau$ in Eq. (19) gives a negligibly small contribution to the material's hardening as $\tau = 2$ s. As a result, the effect of residual hardening is not observed, which is in full conformity with the experimental record.

6 Conclusion

In this study, acoustic temporary softening and acoustic residual hardening during vibration-assisted plastic deformation were modeled. The model was developed based on the synthetic theory of irrecoverable deformation. Analytical results showed good agreement with experimental data. We inserted two terms into the plastic flow rule that determine the deformation behavior of the material both during and after sonication. The first term reflects two opposing processes that occur during acoustoplasticity-accumulation and dynamic annealing of defects-while the latter plays a dominant role in overall deformation (transient softening).

The second process describes how the defect structure of the material affects further deformation of the material after annealing (residual softening or hardening). Although we are limited to the case of residual softening in this paper, our future research will focus on further extending the synthetic theory to capture both effects.

Acknowledgment

The research was conducted in the Doctoral School on Materials Science and Technologies, Obuda University (Hungary). The authors express thanks to Prof. M. Reger for many valuable conversations on the topics presented in this article.

References

[1] G. Malygin, "Acoustoplastic effect and the stress superimposition mechanism," *Physics of the Solid State*, vol. 42, pp. 72-78, 2000, https://doi.org/10.1134/1.1131170.

[2] I. Lum, H. Huang, B. Chang, M. Mayer, D. Du, Y. Zhou, "Effects of superimposed ultrasound on deformation of gold," *Journal of Applied Physics*, vol. 105, 024905. 2009, https://doi.org/10.1063/1.3068352

[3] Y. Daud, M. Lucas, Z. Huang, "Modelling the effects of superimposed ultrasonic vibrations on tension and compression tests of aluminium," *Journal of Materials Processing Technology*, vol. 186, pp. 179-190, 2007, https://doi.org/10.1016/j.jmatprotec.2006.12.032

[4] A. Deshpande, A. Tofangchi, K. Hsu, "Microstructure evolution of Al6061 and copper during ultrasonic energy assisted compression," *Materials Characterization*, vol. 153, pp. 240-250, 2019, https://doi.org/10.1016/j.matchar.2019.05.005

[5] H. Huang, A. Pequegnat, B. Chang, M. Mayer, D. Du, Y. Zhou, "Influence of superimposed ultrasound on deformability of Cu", *Journal of Applied Physics*, vol. 106, 113514, 2009, https://doi.org/10.1063/1.3266170

[6] X. Wang, Z. Qi, W. Chen, "Investigation of mechanical and microstructural characteristics of Ti–45Nb undergoing transversal ultrasonic vibration-assisted upsetting", Materials Science and Engineering: A, 813, 141169, 2021. https://doi.org/10.1016/j.msea.2021.141169

[7] G. Shao, H. Li, M. Zhan, "A Review on Ultrasonic-Assisted Forming: Mechanism, Model, and Process", Chinese Journal of Mechanical Engineering, vol. 34, pp. 1-24, 2021. https://doi.org/10.1186/s10033-021-00612-0

[8] A. Deshpande, K. Hsu, "Acoustic energy enabled dynamic recovery in aluminium and its effects on stress evolution and post-deformation microstructure," *Materials Science and Engineering: A*, vol. 711, pp. 62-68, 2018, https://doi.org/10.1016/j.msea.2017.11.015

[9] A.V. Kulemin, *Ultrasound and Diffusion in Metals*, Metallurgia Publ., Moscow, 1978.

[10] A. Rusinko, "Analytical description of ultrasonic hardening and softening," *Ultrasonics*, vol. 51, pp. 709-714, 2011, https://doi.org/10.1016/j.ultras.2011.02.003

[11] Z. Yao, G. Kim, Z. Wang, L. Faidley, Q. Zou, D. Mei, Z. Chen, "Acoustic softening and residual hardening in aluminum: modeling and experiments," *International Journal of Plasticity*, vol. 39, pp. 75-87, 2012, https://doi.org/10.1016/j.ijplas.2012.06.003

[12] A. Rusinko, K. Rusinko, *Plasticity and creep of metals*. Springer Science & Business Media, 2011, doi 10.1007/978-3-642-21213-0

[13] S. Bagherzadeh, K. Abrinia, K. "Effect of ultrasonic vibration on compression behavior and microstructural characteristics of commercially pure aluminum," *Journal of Materials Engineering and Performance*, vol 24, pp. 4364-4376, 2015, https://doi.org/10.1007/s11665-015-1730-8

[14] U. Geibler, M. Schneider-Ramelow, H. Reichl, "Hardening and softening in AlSi1 bond contacts during ultrasonic wire bonding," *IEEE Transactions on Components and Packaging Technologies*, vol. 32, pp. 794-799, 2009, 10.1109/TCAPT.2008.2009930

[15] H. Zhou, H. Cui, Q. Qin, "Influence of ultrasonic vibration on the plasticity of metals during compression process," *Journal of Materials Processing Technology*, vol. 251, pp. 146-159, 2018, https://doi.org/10.1016/j.jmatprotec.2017.08.021

[16] R. Fitzpatrick, *Oscillations and waves: an introduction*, CRC Press, 2018.

[17] N. Tyapunina, V. Blagoveshchenskii, G. Zinenkova, Y. Ivashkin, "Characteristics of plastic deformation under the action of ultrasound" *Soviet Physics Journal*, vol. 25, pp. 569-578, 1982.